Confinement-Induced Resonances in Low-Dimensional Quantum Systems

Elmar Haller,[1] Manfred J. Mark,[1] Russell Hart,[1] Johann G. Danzl,[1] Lukas Reichsöllner,[1] Vladimir Melezhik,[2]
Peter Schmelcher,[3] and Hanns-Christoph Nägerl[1]

[1]*Institut für Experimentalphysik and Zentrum für Quantenphysik, Universität Innsbruck, Technikerstraße 25, 6020 Innsbruck, Austria*
[2]*Bogoliubov Laboratory of Theoretical Physics, Joint Institute for Nuclear Research, Dubna, 141980 Dubna, Russia*
[3]*Zentrum für Optische Quantentechnologien, Universität Hamburg, Luruper Chaussee 149, 22761 Hamburg, Germany*
(Received 19 February 2010; published 14 April 2010)

We report on the observation of confinement-induced resonances in strongly interacting quantum-gas systems with tunable interactions for one- and two-dimensional geometry. Atom-atom scattering is substantially modified when the *s*-wave scattering length approaches the length scale associated with the tight transversal confinement, leading to characteristic loss and heating signatures. Upon introducing an anisotropy for the transversal confinement we observe a splitting of the confinement-induced resonance. With increasing anisotropy additional resonances appear. In the limit of a two-dimensional system we find that one resonance persists.

Low-dimensional systems have recently become experimentally accessible in the context of ultracold quantum gases. For a two-dimensional (2D) geometry, the Berezinskii-Kosterlitz-Thouless (BKT) transition has been observed [1], and in one dimension the strongly correlated Tonks-Girardeau (TG) [2–6] and super-Tonks-Girardeau (STG) gases [6] have been realized. In these experiments steep optical potentials freeze out particle motion along one or two directions and restrict the dynamics to a plane or to a line. Such quasi-2D or quasi-1D systems can be realized with ultracold gases when the kinetic and the interaction energy of the particles are insufficient to transfer the particles to transversally excited energy levels. Whereas the confinement removes motional degrees of freedom, it also provides an additional structure of discrete energy levels that can be used to modify scattering along the unconfined direction and by this to effectively control the interaction properties of the low-dimensional system [7–9]. In this Letter, we investigate the few-body scattering processes that give rise to the capability to tune interactions and hence to drastically alter the properties of low-dimensional many-body quantum systems [6].

In three-dimensional (3D) geometry magnetically induced Feshbach resonances (FBRs) [10] allow tuning of the interparticle interaction strength. A FBR occurs when the scattering state of two atoms is allowed to couple to a bound molecular state. Typically, the scattering state and bound state are brought into degeneracy by means of the magnetically tunable Zeeman interactions. For particles in 1D and 2D geometry a novel type of scattering resonance occurs. Coupling between the incident channel of two incoming particles and a transversally excited molecular bound state generates a so-called confinement-induced resonance (CIR) [7–9,11–13]. A CIR occurs when the 3D scattering length a_{3D} approaches the length scale that characterizes the transversal confinement, i.e., the har-

monic oscillator length $a_\perp = \sqrt{\hbar/(m\omega_\perp)}$ for a particle with mass m and transversal trapping frequency $\omega_\perp$. This causes the 1D coupling parameter $g_{1D} = \frac{2\hbar^2 a_{3D}}{ma_\perp^2} \frac{1}{1-Ca_{3D}/a_\perp}$ to diverge at $a_\perp = Ca_{3D}$, where $C = 1.0326$ is a constant [7,9]. The CIR allows tuning of interactions from strongly repulsive to strongly attractive and thus represents a crucial ingredient for the control of interactions in a low-dimensional system. Modification of scattering properties due to confinement has been measured near a FBR for fermions [14], and, recently, a CIR has been observed for a strongly interacting 1D quantum gas of bosonic Cs atoms and was used to drive the crossover from a TG gas with strongly repulsive interactions to an STG gas with strongly attractive interactions [6]. Here, for an ultracold quantum gas of Cs atoms with tunable interactions, we study the properties of CIRs by measuring particle loss and heating rate and, in particular, confirm the resonance condition $a_\perp = Ca_{3D}$ for symmetric 1D confinement. For the case of transversally anisotropic confinement we find that the CIR splits and, to our surprise, persists for positive a_{3D} even when the anisotropy reaches the limit of a 2D system.

Figure 1(a) reviews the basic mechanism that causes a CIR for zero collisional energy in one dimension [9]. It is assumed that in three dimensions the scattering potential supports a single universal bound state for strong repulsive interactions (dotted line) [10]. The point where the incoming channel of two colliding atoms and the universal dimer state are degenerate marks the position of a 3D FBR (triangle). In one dimension, strong transversal confinement shifts the zero energy of the incoming channel (middle dashed line) and introduces a transversally excited state (upper dashed line). As a result of the strong confinement, the universal dimer state with binding energy E_B (lower solid line) exists also for attractive interactions [15] whereas the original 3D FBR has disappeared. Instead, there is a CIR (star) when the incoming scattering channel
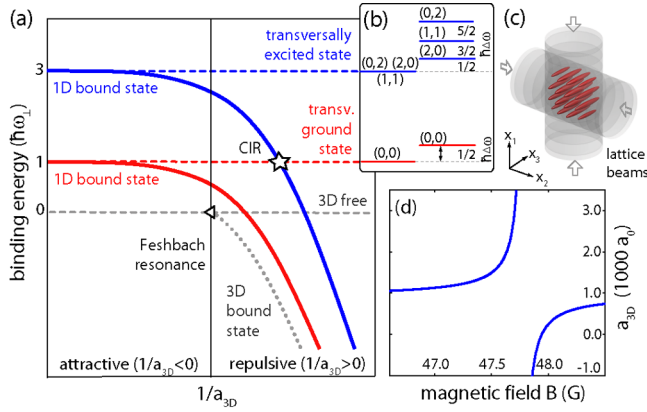
FIG. 1 (color online). (a) Illustration of the mechanism responsible for a CIR; see Ref. [9] and text for details. The energy levels near a scattering resonance are plotted as a function of $1/a_{3D}$. The CIR occurs for $Ca_{3D} = a_\perp$ when scattering atoms are allowed to couple to transversally excited bound states. (b) indicates the shift and splitting for anisotropic confinement characterized by $\Delta\omega$. (c) Experimental configuration. Two laser beams create an optical lattice that confines the atoms to an array of approximately 3000 independent, horizontally oriented elongated 1D tubes. (d) Tuning of a_{3D} is achieved by means of a FBR with a pole at $B = 47.78(1)$ G [18].

becomes degenerate with the transversally excited molecular bound state (upper solid line). It is assumed that the binding energy of this state is also E_B, shifted by $2\hbar\omega_\perp$ [7]. In more detail, as depicted in Fig. 1(b), we assume that the energy levels of noninteracting atoms, as a result of cylindrically symmetric transversal confinement, can be approximated by those of a 2D harmonic oscillator with $E_{n_1,n_2} = \hbar\omega_\perp(n_1 + n_2 + 1)$ and quantum numbers n_1 and n_2 belonging to the two Cartesian directions. Scattering atoms [16] in the transversal ground state $(0,0)$ can couple to the excited states (n_1, n_2) if the parity of the total wave function is preserved [12]. The energetically lowest allowed excited states are threefold degenerate with an energy $E = 3\hbar\omega_\perp$ and with quantum numbers $(1,1)$, $(2,0)$, and $(0,2)$. For the transversally symmetric confinement, they contribute towards a single CIR [9]. However, the contribution of the state $(1,1)$ is negligible due to the zero contact probability of the atoms and the short-range character of the interatomic interaction. Unequal transversal trapping frequencies ω_1 and $\omega_2 = \omega_1 + \Delta\omega$ lift this degeneracy and shift the energy levels according to $E_{n_1,n_2} = \hbar\omega_1(n_1 + n_2 + 1) + \hbar\Delta\omega(n_2 + 1/2)$. One thus expects a splitting of the CIR.

We start from a tunable Bose-Einstein condensate (BEC) of 1.0 to 1.4×10^5 Cs atoms in the energetically lowest hyperfine sublevel [17] confined in a crossed-beam optical dipole trap and levitated against gravity by a magnetic field gradient of $|\nabla B| \approx 31.1$ G/cm. Tunability of a_{3D} is given by a FBR as shown in Fig. 1(d) with its pole at $B_0 = 47.78(1)$ G and a width of 164 mG [17,18]. The BEC is produced at $a_{3D} \approx 290a_0$. We load the atoms within 300 ms into an optical lattice, which is formed by two

retroreflected laser beams at a wavelength of $\lambda = 1064.49(1)$ nm one propagating horizontally as illustrated in Fig. 1(c). These lattice beams confine the atoms to an array of approximately 3000 horizontally oriented, elongated 1D tubes with a maximum occupation of 60 atoms at a linear peak density of approximately $n_{1D} \approx 2/\mu$m. Weak longitudinal confinement results from the Gaussian-shaped intensity distribution of the beams. We raise the lattice to a depth of typically $V = 30E_R$, where $E_R = h^2/(2m\lambda^2)$ is the photon recoil energy. At this depth, the resulting transversal and longitudinal trap frequencies are $\omega_\perp = 2\pi \times$ 14.5 kHz and $\omega_\parallel = 2\pi \times 16$ Hz and we then have $a_\perp \approx 1370a_0$. After loading we slowly ramp down $|\nabla B|$ in 50 ms and adiabatically increase a_{3D} to 915 a0 in 100 ms to create a TG gas with well-defined starting conditions near the CIR [6]. To detect the CIR as a function of B, manifested by a loss resonance, we quickly set B in less than 200 μs to the desired value, wait for a hold time of typically $\tau = 200$ ms, and then measure the number N of remaining atoms by absorption imaging. For this, we relevitate the atoms, ramp down the lattice beams adiabatically with respect to the lattice band structure, and allow for 50 ms of levitated expansion and 2 ms time of flight. Note that τ is chosen to be much longer than the lifetime of the STG phase [6].

We observe the CIR in the form of an atomic loss signature as shown in Fig. 2. We attribute the loss near the resonance to inelastic three-body collisions [19], which lead to molecule formation and convert binding energy into kinetic energy, causing trap loss and heating, similar to the processes observed near a FBR [10]. In Fig. 2(a) the CIR can be identified as a distinct "edge" for the atom number N. Initially, in the TG regime losses are greatly suppressed, but increase rapidly on the attractive side of the CIR. N drops to a minimum when B is increased and then recovers somewhat. A clear shift of the loss signature to lower values for B and hence lower values for a_{3D} can be discerned when the confinement is stiffened. When we identify the position of the edge with the position of the CIR, we find good agreement with the analytical result $Ca_{3D} = a_\perp$ as shown in Fig. 2(b). As we have no theoretical description of the detailed shape of the loss resonance, we also plot, for comparison, the position of the minimum, which is shifted accordingly.

In Fig. 2(c) we juxtapose the loss and the heating rate that we measure in the vicinity of the CIR. For this, we measure the increase of the release energy within the first 100 ms. After holding the atoms for time τ at a given value of B, we decrease a_{3D} back to 250 a_0 in 20 ms, switch off the lattice potential and determine the release energy in the direction of the tubes from the momentum distribution in free space expansion. We observe an increase for the heating rate when the CIR is crossed. From a low value of 10 nK/s in the TG regime it rises to a maximum of approximately 150 nK/s and then drops to settle at some intermediate value. The position of the maximum agrees
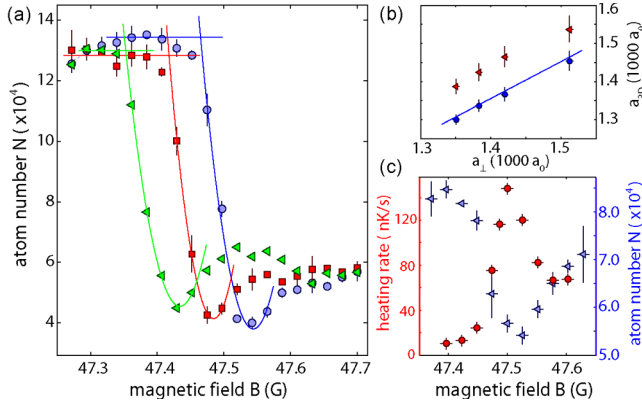
FIG. 2 (color online). Particle loss and heating rates in the vicinity of a CIR. (a) The number N of remaining atoms after $\tau = 200$ ms shows a distinct drop (edge) when B is scanned across the CIR. A clear shift of the position of the edge to lower values for B can be observed when the transversal confinement is stiffened, $\omega_\perp = 2\pi \times (0.84, 0.95, 1.05) \times 14.2(2)$ kHz (circles, squares, triangles). (b) Position of the edge (circles) as determined from the intersection point of a second-order polynomial fit to the minimum for N and the initial horizontal baseline as shown in (a), converted into values for a_{3D}. For comparison, the position of the minimum (triangles) is also shown. The solid line is given by $Ca_{3D} = a_\perp$. (c) Heating rates near the CIR (circles). For comparison, N is also shown (triangles). Here, $\omega_\perp = 2\pi \times 12.0(2)$ kHz. All error bars reflect 1σ statistical uncertainty.

well with the maximum for atom loss. We check that the system's increase in energy is sufficiently small so that its 1D character is not lost. The release energy, even at maximal heating, remains below $k_B \times 30$ nK, which is far below the energy spacing of the harmonic oscillator levels, $\hbar\omega_\perp \approx k_B \times 600$ nK.

We now examine 1D systems with transversally anisotropic confinement. Starting from a lattice depth of $V = 25E_R$ along both transversal directions, yielding $\omega_\perp = \omega_1 = \omega_2 = 2\pi \times 13.2(2)$ kHz, we increase the horizontal confinement to frequencies up to $\omega_2 = 2\pi \times 16.5(2)$ kHz, corresponding to a lattice depth of $39E_R$, while keeping the depth of the vertical confinement constant. Figure 3(a) shows a distinct splitting of the original CIR into two loss resonances, CIR_1 and CIR_2. The splitting increases as the anisotropy is raised. In Fig. 3(b) we plot the 3D scattering length values $a_{3D,1}$ and $a_{3D,2}$ that we associate with the positions of CIR_1 and CIR_2 as a function of the frequency ratio ω_2/ω_1. For this, as it becomes difficult to assign an edge to both of them, we simply determine the associated atom number minima and subtract a constant offset of $88(7)a_0$ as determined from the measurement shown in Fig. 2(b). One of the resonances, CIR_2, exhibits a pronounced shift to smaller values for a_{3D} as the horizontal confinement is stiffened. The second resonance, CIR_1, shows a slight shift towards higher values for a_{3D}. We now use the lifting of the degeneracy for the energy levels as indicated in Fig. 1(b) to model the observed splitting of the CIR. We assume that the implicit equation

$\zeta(1/2, -E_B/(2\hbar\omega_\perp) + 1/2) = -a_\perp/a_{3D}$ for the binding energy E_B [9] remains approximately valid for sufficiently small $\Delta\omega$, taking $\omega_\perp = \omega_1$. Here, ζ is the Hurwitz zeta function. We translate the scattering length values $a_{3D,1}$ and $a_{3D,2}$ into binding energies and calculate the energy difference $\Delta E_B = E_B(a_{3D,1}) - E_B(a_{3D,2})$, shown in Fig. 3(c). While this model does not explain the upward deviation seen for CIR_1, the difference ΔE_B is in reasonable agreement with the expected energy shift caused by the shifts of the excited harmonic oscillator states ($E_{0,2} - E_{2,0}$) = $2\hbar\Delta\omega$ [solid line in Fig. 3(c)]. We thus attribute CIR_2 to the stiffened confinement along the horizontal direction and hence to state (0,2), while CIR_1 corresponds to the unchanged confinement along the vertical direction and hence to state (2,0).

We observe the appearance of additional structure in the measured loss curves when we increase the transversal anisotropy by weakening the confinement along one axis, here along the vertical direction. Figure 4(a) shows the atom number after $\tau = 300$ ms for trapping frequency ratios ω_1/ω_2 from 0.67 to 0.45. Multiple loss resonances appear close to the position of CIR_1. The number of resonances increases and the positions shift continuously as the confinement is weakened. We speculate that those resonances are a result of a coupling to additional excited states, resulting in a multichannel scattering situation. Also
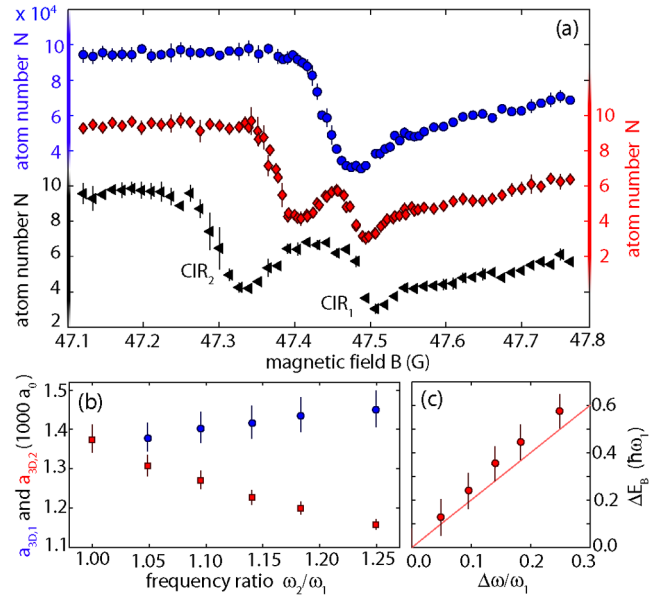

FIG. 3 (color online). Splitting of a CIR for a 1D system with transversally anisotropic confinement. (a) As the horizontal confinement is stiffened, $\omega_2/\omega_1 = 1.00, 1.10, 1.18$ (circles, diamonds, triangles) for $\omega_1 = 2\pi \times 13.2(2)$ kHz, the CIR splits into CIR_1 and CIR_2. (b) Position of CIR_1 ($a_{3D,1}$, circles) and CIR_2 ($a_{3D,2}$, squares) as a function of the frequency ratio ω_2/ω_1. (c) Binding energy difference ΔE_B as determined from the implicit equation (see text) in comparison to the expectation from the simple harmonic oscillator model (solid line).
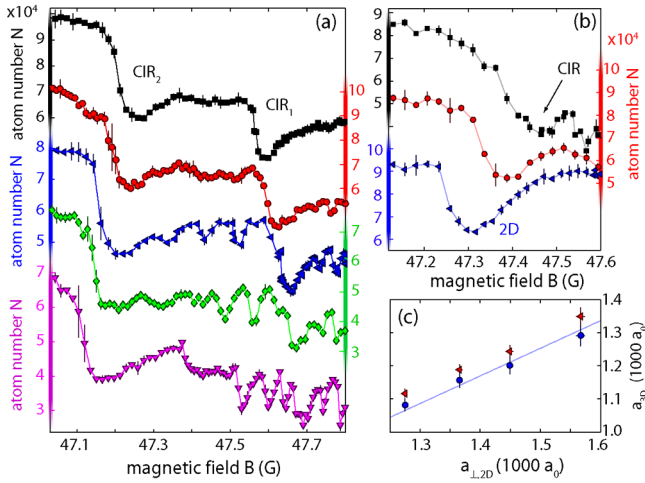
FIG. 4 (color online). (a) Appearance of additional structure in the vicinity of CIRs for strongly anisotropic transversal confinement. The trap frequencies are $\omega_2 = 2\pi \times 16.6(2)$ kHz and $\omega_1/\omega_2 = 0.67, 0.60, 0.53, 0.49, 0.45$ from top to bottom. (b) Transition from 1D to 2D confinement. As the horizontal lattice is ramped down, CIR_2 shifts and persists, while CIR_1 disappears ($\omega_1 = 2\pi \times 13.0(2)$ kHz and $\omega_2/\omega_1 = 0.58, 0.42, 0.00$ for squares, circles, and triangles). (c) Scaling of the CIR's position in 2D, in analogy to the 1D case shown in Fig. 2(b). The position of the CIR as determined from the edge (circles) and, alternatively, from the minimum in atom number (triangles) shifts to lower values for a_{3D} as the confinement is stiffened and $a_{\perp,2D}$ is reduced. The solid line is a linear fit according to $C_{2D}a_{3D} = a_{\perp,2D}$ with $C_{2D} = 1.19(3)$.

the weakening of the confinement could induce sufficient anharmonicity to allow for violation of the parity rule [20].

Surprisingly, we find that one of the CIRs persists in the limit of a 2D system. Previous theoretical studies on 2D systems have predicted the appearance of a CIR for negative a_{3D}, but not for positive a_{3D} [13,21]. In the experiment, we reduce the horizontal confinement while keeping the vertical confinement constant to probe the transition from the array of tubes to a stack of pancake-shaped, horizontally oriented 2D systems. Trapping in the horizontal direction is still assured, now by the Gaussian profile of the vertically propagating laser beam, for which $\omega_2 = 2\pi \times 11$ Hz. Figure 4(b) shows that the CIR associated with the tight confinement shifts to lower values for B and hence for a_{3D} as the horizontal confinement is weakened. In the limit of 2D confinement, one of the CIRs, and in fact all the additional structure observed above, have disappeared, but one resonance persists. To check that the observed resonance is indeed the result of the 2D confinement, we vary the confinement along the tight vertical direction. Figure 4(c) plots the positions of edge and minimum of the loss signature as a function of $a_{\perp,2D}$, the confinement length associated with this direction. When we again associate the edge with the pole of the resonance, we obtain $C_{2D}a_{3D} = a_{\perp,2D}$ with $C_{2D} = 1.19(3)$, where C_{2D} is a scaling factor similar to C for the 1D case. Further scattering

experiments are needed to elucidate the energy dependence of this 2D scattering resonance.

In summary, we have investigated the properties of CIRs, which appear in low-dimensional quantum systems as a result of tight confinement and which replace "conventional" 3D Feshbach resonances to tune the effective atomic interaction strength. We observed a splitting of the CIR for anisotropic transversal confinement, the appearance of multiple resonances for strongly anisotropic confinement, and the survival of one resonance for positive a_{3D} in the limit of 2D confinement. We expect that CIRs will not only be used in 1D geometry to tune the effective interaction strength as recently demonstrated [6], but also in 2D geometry and mixed dimensions [22] for the study of strongly interacting quantum systems.

[1] Z. Hadzibabic et al., Nature (London) **441**, 1118 (2006).
[2] M. Girardeau, J. Math. Phys. (N.Y.) **1**, 516 (1960).
[3] T. Kinoshita, T. Wenger, and D. S. Weiss, Science **305**, 1125 (2004).
[4] B. Paredes et al., Nature (London) **429**, 277 (2004).
[5] N. Syassen et al., Science **320**, 1329 (2008).
[6] E. Haller et al., Science **325**, 1224 (2009).
[7] M. Olshanii, Phys. Rev. Lett. **81**, 938 (1998).
[8] D. S. Petrov, M. Holzmann, and G. V. Shlyapnikov, Phys. Rev. Lett. **84**, 2551 (2000).
[9] T. Bergeman, M. G. Moore, and M. Olshanii, Phys. Rev. Lett. **91**, 163201 (2003).
[10] C. Chin et al., arXiv:0812.1496v2 [Rev. Mod. Phys. (to be published)].
[11] E. Tiesinga et al., Phys. Rev. A **61**, 063416 (2000); V. A. Yurovsky, Phys. Rev. A **71**, 012709 (2005); V. S. Melezhik, J. I. Kim, and P. Schmelcher, Phys. Rev. A **76**, 053611 (2007); S. Saeidian, V. S. Melezhik, and P. Schmelcher, Phys. Rev. A **77**, 042721 (2008).
[12] J. I. Kim, J. Schmiedmayer, and P. Schmelcher, Phys. Rev. A **72**, 042711 (2005).
[13] P. Naidon et al., New J. Phys. **9**, 19 (2007).
[14] K. Günter et al., Phys. Rev. Lett. **95**, 230401 (2005).
[15] H. Moritz et al., Phys. Rev. Lett. **91**, 250402 (2003).
[16] Center-of-mass and relative motion separate for identical particles in a harmonic trap.
[17] T. Kraemer et al., Appl. Phys. B **79**, 1013 (2004).
[18] A. D. Lange et al., Phys. Rev. A **79**, 013622 (2009).
[19] T. Weber et al., Phys. Rev. Lett. **91**, 123201 (2003).
[20] V. Peano et al., New J. Phys. **7**, 192 (2005).
[21] D. S. Petrov and G. V. Shlyapnikov, Phys. Rev. A **64**, 012706 (2001).
[22] G. Lamporesi et al., Phys. Rev. Lett. **104**, 153202 (2010).